Optics Letters

Effect of second order signal–noise interactions in nonlinearity compensated optical transmission systems

Mohammad A. Z. Al-Khateeb,* Mary McCarthy, Christian Sánchez, and Andrew Ellis

Aston Institute of Photonic Technologies (AIPT), Aston University, Birmingham, B4 7ET, UK
**Corresponding author: alkhamaz@aston.ac.uk*

Received 21 January 2016; revised 9 March 2016; accepted 14 March 2016; posted 15 March 2016 (Doc. ID 257891); published 14 April 2016

In this Letter, we theoretically and numerically analyze the performance of coherent optical transmission systems that deploy inline or transceiver based nonlinearity compensation techniques. For systems where signal-signal nonlinear interactions are fully compensated, we find that beyond the performance peak the signal-to-noise ratio degradation has a slope of 3 dB_{SNR}/dB_{Power} suggesting a quartic rather than quadratic dependence on signal power. This is directly related to the fact that signals in a given span will interact not only with linear amplified spontaneous emission noise, but also with the nonlinear four-wave mixing products generated from signal-noise interaction in previous (hitherto) uncompensated spans. The performance of optical systems employing different nonlinearity compensation schemes were numerically simulated and compared against analytical predictions, showing a good agreement within a 0.4 dB margin of error.

OCIS codes: (060.1660) Coherent communications; (060.2330) Fiber optics communications; (060.2360) Fiber optics links and subsystems.

https://doi.org/10.1364/OL.41.001849

As the development of optical long haul transmission systems attempts to accommodate the exponential growth of information capacity demands [1], many fiber nonlinearity compensation techniques have been investigated to enable higher spectral efficiency and/or higher reach. Such links are ultimately limited by amplified spontaneous emission (ASE) noise and the nonlinear Kerr effect [2] in which the highest signal-to-noise ratio (SNR) is achieved by optimizing the optical signal launched power. Nonlinearity compensation techniques have been proposed in the electronic domain [such as digital back-propagation (DBP) [3]] and in the optical domain [such as optical phase conjugation (OPC) [4]]. They can mitigate the impact of deterministic Kerr effects namely the inter and intra channel nonlinear interference [5] leaving the system limited by the nondeterministic Kerr effects due to the influence of polarization mode dispersion (PMD) and signal-noise interactions (known as the Gordon–Mollenauer effect [6] or parametric noise amplification [7]). High levels of PMD can severely degrade the performance of the compensated system, such that the uncompensated signal-signal nonlinearity dominates over the effects of the signal–noise nonlinear Kerr effects [8], but the influence of PMD can be avoided by using either low PMD or polarization maintaining (PM) fibers. In the case of DBP, a closed form approximation of the SNR evolution as a function of the optical signal power has been presented for the signal–noise interaction [8,9] and suggested that the received SNR degrades at a rate of 1 dB_{SNR}/dB_{Power} when operating in the regime of nonlinear signal–noise interaction. Similar results have been formulated for the case of ideal inline OPCs which limit the quadratic growth of nonlinear noise resulting from the signal–noise interaction along the link [7]. However, these and many other numerical results [7–13] show more rapid SNR degradation in the nonlinear regime of up to 3 dB_{SNR}/dB_{Power} which are as yet unexplained.

In this Letter, we propose and validate an accurate closed form SNR expression covering both lumped and ideal Raman amplified optical transmission systems that compensate deterministic nonlinearities using DBP or OPC. The analytical expression considers the nonlinear noise generated from both first-order signal–noise four-wave mixing (FWM), resulting from the signal interaction with the ASE noise, and second-order signal–noise FWM, resulting from the signal interaction with first-order signal–noise products generated from previous uncompensated spans, and a degeneracy factor due to the interchangeability of signal–noise FWM products. To validate the analytical expression, we have conducted numerical simulations of single channel 112 Gbps of polarization multiplexed quadrature phase-shift keying (PM-QPSK) and compared the Q^2 factor of received signals to the analytical results.

Nonlinear optical fiber effects can be represented in terms of FWM applied to small spectral slices of the optical signal spectrum as found in orthogonal frequency-division multiplexing signals [14] or as a continuous integral for Nyquist wavelength-division multiplexed channels [13]. FWM describes the interaction between three tones (f_A, f_B, and f_C) to

generate a fourth tone ($f_{\mathrm{FWM}} = f_A + f_B - f_C$) leading to signal interference which is noise-like if the generating tones may be considered as independent random variables [14]. In the case of a noise field superimposed on optical signal fields, the ensemble average [15] of generated FWM products can be written as

$$P_{\mathrm{FWM}} = (|E_A|^2 + |E_a|^2)(|E_B|^2 + |E_b|^2)(|E_C^*|^2 + |E_c^*|^2)\eta$$
$$= \begin{bmatrix} (P_A P_B P_C) \\ +(P_A P_B P_c) + (P_A P_b P_C) + (P_a P_B P_C) \\ +(P_A P_b P_c) + (P_a P_B P_c) + (P_a P_b P_C) \\ +(P_a P_b P_c) \end{bmatrix} \eta, \quad (1)$$

where E_Y is the optical signal field of tone Y (at f_Y) and E_y is the optical noise field at the same frequency, ($*$ represents conjugation), P is the optical power (equal to $|E|^2$), and η is the FWM efficiency (described for a periodically amplified system in [16]). The first row in the squared bracket of Eq. (1) represents the signal-signal FWM [14], which can be fully compensated by nonlinear compensation techniques; the second row represents nonlinear noise generated from the signal–noise interaction [7–9]; and the third and fourth rows represent the nonlinear phase noise and noise–noise interactions, respectively, and may usually be neglected. From Eq. (1), it is clear that for a typical communication system the net efficiency of any signal–noise interaction is three times the efficiency of the signal-signal interaction. Thus, assuming that all signal fields have the same power and all noise fields have the same power, SNR can be written as

$$\mathrm{SNR} = \frac{I_S}{NI_n + I_S^3 f_A(N) + 3I_S^2 I_n \xi_{\mathrm{PAN}}(N)}, \quad (2)$$

where I_S and I_n are the signal and ASE noise power spectral density added by each amplifier, respectively. The coefficient $f_A(N)$ represents the nonlinear scaling factor for (N) spans with amplification scheme *A (lumped or ideal Raman)* which result from solving the double integral of η over the signal bandwidth (B_W) and the nonlinear scaling factor due to parametric amplified noise (ξ_{PAN}). The nonlinear scaling factor for a link containing N spans has been reported in closed form for the dispersion uncompensated lumped transmission system as [14]

$$f_{\mathrm{Lumped}}(N) = \frac{\gamma^2 N}{\pi\ \alpha|\beta_2|} \log\left(\frac{2\pi^2|\beta_2|B_W^2}{\alpha}\right), \quad (3)$$

where α is the loss coefficient of the fiber, and β_2 is the second-order dispersion of the fiber. If the optical fiber has an intrinsic nonlinear factor of γ_0, then, γ^2 in Eq. (3) can be represented for single polarization system as $\gamma^2 = \gamma_0^2$ and for the dual polarization system (random birefringence fiber) as [15] $\gamma^2 = 8\gamma_0^2/27$. Following the same approach in [14], the nonlinear scaling factor with ideal lossless Raman amplification can be written as

$$f_{\mathrm{Raman}}(N) = 2\frac{\gamma^2 \mathrm{NL}}{\pi|\beta_2|} \log(2\pi^2\ \mathrm{NL}|\beta_2|B_W^2). \quad (4)$$

We note that the primary difference between Eqs. (3) and (4) is the replacement of the effective length ($1/\alpha$, assuming large span length) with the total length (NL) and a factor of increase in interaction strength. Here, we assume ideal compensation of deterministic signal-signal nonlinearity and so we set the noise resulting from signal-signal interactions represented by the second term in the denominator of Eq. (2) to zero.

When considering the first span in a transmission system that has an input signal and linear ASE noise, then the parametric amplified noise nonlinear factor ξ_{PAN} will be equal to the nonlinear scaling factor for a single span $f_A(1)$. The propagation of both signal and ASE noise through the span will produce a nonlinear noise from signal–noise interaction that grows with a rate of 2 $\mathrm{dB/dB_{Signal\_Power}}$; we will call this generated nonlinear noise as first-order signal–noise products. As signal power increases, first-order signal–noise products reach non-ignorable power compared to the linear ASE noise injected at the beginning of the span. As a result, both the linear ASE noise and the first-order signal–noise products must be taken into account when passing to propagate in the next span which allow signals to interact with the linear ASE noise to generate another first-order signal–noise product by the end of the second span, as well as signal interaction with the first-order signal–noise products to generate second-order signal–noise products.

In the case of the multi-span DBP system in Fig. 1, nonlinearity generated from noise field I_n added by the transmitter amplifier is fully compensated by DBP due to the symmetry of signal and ASE noise propagation in both the actual transmission link and the virtual digital propagation constructed at the receiver side; this symmetry is not valid anymore for noise powers added by the three inline amplifiers. Looking at the noise added from inline amplifiers in the DBP system, we can see that the receiver will overcompensate signal propagation with the linear ASE noise to generate first-order signal–noise products [7] (represented in Fig. 1 by green filled triangles and the first term in the numbered expressions below the figure); furthermore, the receiver will overcompensate signal propagation with first-order signal–noise products to generate second-order signal–noise products (represented in Fig. 1 by black arrows and the second term in the numbered expressions below the figure). The most

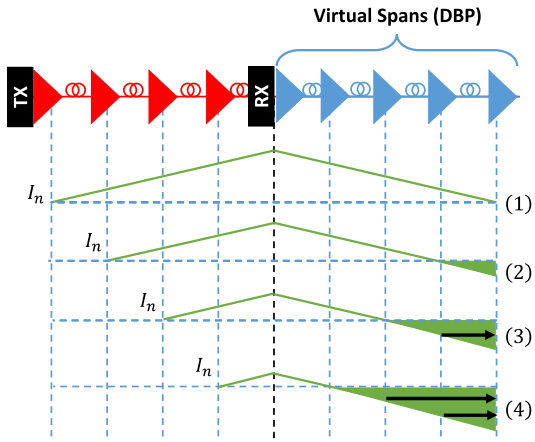

Fig. 1. Nonlinear signal–noise interactions accumulation along the nonlinearity DBP compensated optical transmission link. The red triangles represent inline amplifiers that inject linear ASE noise while the blue triangles are ideal DBP amplifiers that do not introduce any noise. The blue colored fibers in the receiver side represent fibers with the negative values γ and β_2 of the red fiber. The green solid lines represent the power evolution of the signal interaction with noise, the filled green triangles represent the first-order signal–noise products, and the black arrows represent second-order signal–noise products.

efficient multi-OPC system divides the optical transmission link into equally sized segments, minimizing signal–noise interactions while fully recovering signal–signal interference. In such a symmetric system any OPC placed in between two consecutive segments can fully recover signal–signal interference generated in those segments, and adds no net nonlinear interference for signals injected into the first of those segments. Consequently, from Fig. 1, we can see that the parametric amplified noise (scaling factor ξ_{PAN}) in the DBP system can be found by a single summation of all the first-order signal–noise interactions resulting from each ASE noise power added by each amplifier in the system, as well as a double summation to calculate the second-order signal–noise interaction where the internal summation determines the power of the second-order signal–noise interaction products from the ASE noise power added by a specific inline amplifier and the outer summation; the outer summation adds all such products. In this Letter, we place OPCs fully symmetrically in the system to have N_s spans (single segment) between the transmitter and the first OPC in the link, between the last OPC and receiver, and between any two consecutive OPCs [7]. Alternative approaches include adding half a segment of nonlinear digital processing at the transmitter and receiver, boosting the performance by 1.5 dB [7], or by placing $2N_s$ spans (two segments) between any two consecutive OPCs [17] resulting in the same system performance as considered here for a similar segment size (N_s). The factor of ξ_{PAN} can be written for a generic DBP or multi-OPC system (ideal OPCs) as

$$\xi_{\mathrm{PAN}} = N_{\mathrm{even}}\left\{\sum_{x=1}^{N_S}\left(f(x)+\left[3I_S^2 f(1)\sum_{y=1}^{x-1}f(y)\right]\right)\right\} + N_{\mathrm{odd}}\left\{\sum_{x=1}^{N_S}\left(f(N_S-x)+\left[3I_S^2 f(1)\sum_{y=1}^{x-1}f(N_S-y)\right]\right)\right\}, \tag{5}$$

where N_{even} and N_{odd} are, respectively, the number of even and odd indexed link segments that result in undercompensated and overcompensated signal–noise interactions in an OPC compensated system, and N_s is the number of spans within the segment ($N_s = N/(N_{\mathrm{OPC}}+1)$ for the OPC placement configuration used here, or $N_s = N/(2N_{\mathrm{OPC}})$ if every second OPC is omitted [17]). Following the same approach of [7] which only considers first-order signal–noise interaction, the expression in Eq. (5) takes into account the second-order signal–noise products (in the squared bracket) representing a new nonlinear factor that leads to noise enhancement of 4 $\mathrm{dB/dB_{signal\ power}}$. In the case of DBP for a lossy optical fiber transmission system ($N_{\mathrm{odd}} = 1$, $N_{\mathrm{even}} = 0$, $N_s = N$, and $f_{\mathrm{Lumped}}(N) = Nf_{\mathrm{Lumped}}(1)$), the SNR of the systems limited by the nonlinear signal–noise interaction can be written in a simple closed form as

$$\mathrm{SNR} = \frac{I_S}{NI_n + \frac{3N(N+1)}{2}I_S^2 I_n f_{\mathrm{lumped}}(1)[1+(N-1)I_S^2 f_{\mathrm{lumped}}(1)]}. \tag{6}$$

To verify the previous analytical Eqs. (2)–(6), we have simulated (using VPITransmissionMaker 9.3 and Matlab) a 112 Gbps PM-QPSK system operating at 1550 nm carrying two pseudo random bit sequences (PRBS) on each polarization. The transmitted signals were Nyquist pulse shaped with a roll off factor of 0.01, and the total number of transmitted bits was 2×10^{15} bits per polarization. The modulated optical signals have been simulated with 16 samples per symbol, and we have simulated two types of systems: system A propagates signals into 12×100 km dispersion uncompensated fiber ($\alpha = 0.2$ dB/km) with an erbium-doped fiber amplifier installed at the end of each span that have noise figures (NF) of 6 dB, generating a noise power spectral density of 5.1×10^{-17} W/Hz; system B propagates the signals in 12×100 km lossless fiber ($\alpha = 0$ dB/km) with noise power spectral density injected by the end of each span equal to 1.1×10^{-17} W/Hz. This noise power spectral density was selected so that system B achieves the same optimum received SNR as system A in the case of an electronic dispersion compensated (EDC) system. The fiber in both systems had a nonlinear factor $\gamma_0 = 1.33$ $(\mathrm{W.km})^{-1}$, chromatic dispersion of 16 ps/nm/km, zero PMD, and the step size of the fiber was calculated with a maximum nonlinear phase change of 0.01 degrees. The ideal OPC modules were simulated by conjugating the optical field.

At the receiver side, signals were coherently detected with eight samples per symbol to enable DBP to fully compensate the deterministic signal–signal interference, convergence tests have been conducted to conclude that sampling rate over six samples per symbol will have the same maximum Q^2 factor. Coherently detected signals were passed to the DSP module, implemented in Matlab, to compensate for dispersion (in the case of EDC), or to perform DBP with 120 steps/span (in the case of DBP nonlinearity compensated system), or nothing (in the case of OPC nonlinearity compensated system). The signals then were down-sampled to two samples per symbol; then passed to a phase recovery block which was performed using Viterbi–Viterbi algorithm with an averaging window of 21. The Q^2 (which is equal to SNR in our case since we have used the QPSK modulation format) of received signals were calculated from the error vector magnitude (EVM). System A uses DBP to fully compensate signal-signal nonlinear interactions; the OPC solution will not be used in this system since power profile symmetry condition is not satisfied to allow full compensation of signal-signal nonlinear interactions. System B deploys different ideal nonlinearity compensation techniques: DBP, 1-OPC, 3-OPCs, and 11-OPCs.

The results from the simulation of system A, in Fig. 2, show that the DBP of the lumped optical transmission can introduce 7.95 dB improvement of Q^2 and 8.8 dB improvement in optimal launched signal power; the numerical simulations show a good matching (with ± 0.2 dB error) with the theory that considers both first-order and second-order signal–noise products leading to the SNR being degraded in the nonlinear regime according to a fourth-order rational polynomial describing the transition from the linear regime to the nonlinear regime generated from the nonlinear noise due to signal–noise interactions. First-order interactions would be expected to increase the noise at a rate of 2 $\mathrm{dB_{Noise}/dB_{Sig}}$ predicting a slope of −1 $\mathrm{dB_{SNR}/dB_{Sig}}$ in a nonlinear threshold curve, such as Fig. 2, which is rarely observed [7–13]; however, adding second-order interactions adds a term to the noise which grows as 4 $\mathrm{dB_{Noise}/dB_{Sig}}$ predicting a slope in the highly nonlinear regime which approaches −3 $\mathrm{dB_{SNR}/dB_{Sig}}$. For a system employing lumped amplification, the difference in optimum Q^2 when considering both first- and second-order signal–noise products and when considering only first-order signal–noise products is 0.7 dB, regardless of the number of amplifiers in the links which can be identified by differentiating the equations of both approaches with respect to number of spans.

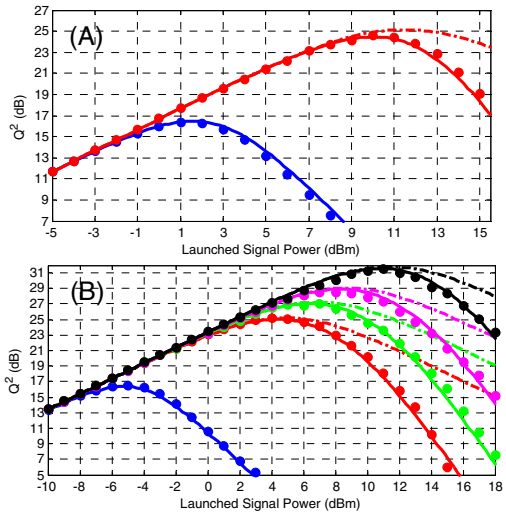

Fig. 2. Q^2 factor, as a function of optical signal launched power, for system (A) and system (B). Theory considering the first- and second-order signal–noise products (solid line), theory considering only the first-order signal–noise products (dashed line), and simulation results (dots). EDC system without nonlinearity compensation (blue), DBP (red), 1-OPC (green), 3-OPCs (purple), and 11-OPCs (black).

The simulation results of ideal lossless Raman nonlinearity compensated transmission (system B) displayed in Fig. 2(B), again, show a good agreement (within ±0.15 dB error) with the theoretical prediction that considers both the first-order and second-order signal–noise products. The results show that DBP can introduce only 8.5 dB of Q^2 improvement and 9.35 dB of optimal launched signal power; in this system, we had an extra 0.4 dB of Q^2 improvement compared to system A which relates to the effective length inside the log in Eq. (4) that slightly reduces ξ_{PAN} of system B compared to the equivalent ξ_{PAN} of system A. In the case of OPC-based nonlinearity compensated transmission system, the optimum Q^2 improvements for a different number of OPCs can be represented either using first-order signal–noise interaction or both first- and second-order signal–noise interaction with a difference of 0.3 dB, but using the second approach will give a more accurate approximation of the nonlinear regime of signal–noise interaction. For the theoretical evaluation of 11 OPCs (OPC per span with segment size of one span), we have added second-order signal–noise interaction as (which can be derived by simple integration of first-order signal–noise interaction over span length):

$$I_{\mathrm{PAN}}^{\mathrm{2nd\text{-}Order}} = \frac{I_S^4 I_n}{6}\left(\frac{2\gamma^2 L}{\pi|\beta_2|}\right)^2 \log(2\pi^2 L|\beta_2|B_w^2). \qquad (7)$$

In Fig. 3, we show the effect the number of spans; we have plotted the Q^2 degradation as a function of distance for a mid-link OPC transmission link (system B) given a constant signal power of 10 dBm. We can see that at low distance, where the linear ASE noise power restricts performance, the systems have the same performance for both cases of the SNR approximations with or without considering the second-order signal–noise products. As the distance increases, nonlinear signal–noise interactions start to dominate the degradation of performance, and second-order signal–noise products will show a higher impact compared to the first-order signal–noise

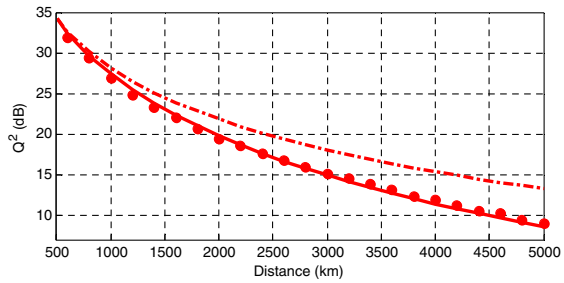

Fig. 3. Q^2 as a function of the optical link distance for mid-link OPC (System B). Theory considering the first-order and second-order signal–noise products (solid line), theory considering only the first-order signal–noise products (dashed line), and simulation results (dots).

products. Again, simulation results show a good agreement with the analytical expression that considers both first- and second-order signal–noise interactions.

In conclusion, we have explained for the first time, to the best of our knowledge, the reasoning behind the sudden SNR degradation in the nonlinear regime [7–13] of nonlinearity compensated transmission systems (deploying DBP or ideal in-line OPCs). We have introduced analytical expressions defining the evolution of parametric amplified noise considering both first- and second-order signal–noise interactions along different optical transmission systems. Our analytics show an accurate (within 0.4 dB error) representation of the nonlinear regime of the nonlinearity compensated systems.

Funding. Engineering and Physical Sciences Research Council (EPSRC) (EP/J017582/1, EP/L000091/1).

Acknowledgment. We thank Prof. Keith Blow and Son Le Thai for useful discussions and Filipe Ferreira for technical support. Original data for this work is available through Aston Research Explorer (http://dx.doi.org/10.17036/421bac57-8e97-43e9-848c-88c604fb0069).

REFERENCES

1. A. D. Ellis, Nonlinear Opt. Appl. VI **8434**, 84340H (2012).
2. P. P. Mitra and J. B. Stark, Nature **411**, 1027 (2001).
3. X. Li, X. Chen, G. Goldfarb, E. Mateo, I. Kim, F. Yaman, and G. Li, Opt. Express **16**, 880 (2008).
4. A. Yariv, D. Fekete, and D. M. Pepper, Opt. Lett. **4**, 52 (1979).
5. G. P. Agrawal, *Nonlinear Fiber Optics* (Elsevier, 2006).
6. J. P. Gordon and L. F. Mollenauer, Opt. Lett. **15**, 1351 (1990).
7. A. D. Ellis, M. E. McCarthy, M. A. Z. Al-Khateeb, and S. Sygletos, Opt. Express **23**, 20381 (2015).
8. G. Gao, X. Chen, and W. Shieh, Opt. Express **20**, 14406 (2012).
9. D. Rafique and A. D. Ellis, Opt. Express **19**, 3449 (2011).
10. F. Yaman and G. Li, IEEE Photon. J. **2**, 816 (2010).
11. A. D. Ellis, S. T. Le, M. A. Z. Al-Khateeb, S. K. Turitsyn, G. Liga, D. Lavery, T. Xu, and P. Bayvel, *IEEE Photonics Society Summer Topical Meeting Series (SUM)*, Nassau (2015).
12. A. D. Ellis, S. T. Le, M. E. McCarthy, and S. K. Turitsyn, *17th International Conference on Transparent Optical Networks (ICTON)*, Budapest (2015), pp. 1–4.
13. T. Fehenberger and N. Hanik, *Eur. Conf. Opt. Commun. (ECOC)* (2014), pp. 1–3.
14. X. Chen and W. Shieh, Opt. Express **18**, 19039 (2010).
15. W. Shieh and X. Chen, IEEE Photon. J. **3**, 158 (2011).
16. D. A. Cleland, J. D. Cox, and A. D. Ellis, Electron. Lett. **28**, 307 (1992).
17. M. H. Shoreh, J. Opt. Commun. Netw. **6**, 549 (2014).